



A new MEMS based variable capacitor using electrostatic vertical comb drive actuator and auxiliary cantilever beams

Saeid Afrang¹ · Nooshin Nematkhah¹

Received: 30 September 2018 / Accepted: 2 January 2019 / Published online: 23 January 2019
© Springer-Verlag GmbH Germany, part of Springer Nature 2019

Abstract

We have proposed a new wide tunable MEMS variable capacitor. In the proposed structure, an electrostatic vertical comb drive actuator is used to extend the tuning range. Moreover, the auxiliary cantilever-beams are used in the electrostatic comb drive actuator to delay the front sticking (Pull in) and increase the tunability. The effect of lateral gap distance between the fingers in the capacitance tunability is investigated. Not only a full review of electrostatic actuator portion is done but also the electric fields related to lateral gap changes are simulated by COMSOL software and its results are compared with theoretical results as well. The structure is calculated using MATLAB software. To verify, the calculated results are compared with simulated results using Intellisuite software. According to calculation and simulation results the achieved tuning range is 285%.

1 Introduction

MEMS variable capacitors have wide applications in RF circuits for wireless communications such as low-noise voltage-controlled oscillators (VCO's) and high dynamic range filters and have the potential to replace varactor diodes in many RF and microwave applications such as phase shifters and tunable filters. Micromachined variable capacitors are very attractive due to their advantages of low parasitics, large voltage swing and high Q (Nguyen et al. 1998, 2002; Yao et al. 1998, 2000; Dec et al. 2000; Zou et al. 2000; Young et al. 1996; Young et al. 1999; Yao et al. 2000). The main objectives for a micromachined variable capacitor are to achieve low driving voltage, high tuning ratio, and low mechanical noise sensitivity. Micromachined variable capacitors generally fall in two categories those that vary the area and those that vary gap (Li and Tien 2002, Yao et al. 2000, 1998). Often, gap-tuning capacitors are constructed from two surface-micromachined electrostatically-actuated parallel plates. One drawback of this method is that the movable plate can only be actuated one-third of the initial gap distance; beyond this value, the two plates will snap together. In this case, the maximum

theoretical tuning ratio is only 1.5:1. In practice, the tuning range can be even lower because of electrical overshoot or mechanical shock. Although techniques that increase the tuning range have been reported (Dec et al. 2000; Zou et al. 2000), they often do not have tuning ratios large enough for many RF applications, and furthermore, have increased process complexity. Recently, several approaches have been reported to enhance the tuning range of variable capacitors. The approaches involve either parallel plate capacitors and actuators (Mobki et al. 2011; Afrang et al. 2015; Bakri-Kassem et al. 2004a, b; Faheem et al. 2003; Rijks et al. 2004; Bakri-Kassem et al. 2006; Peroulis et al. 2003) or interdigitate capacitors with comb drive actuation mechanisms (Nguyen et al. 2004; Borwick et al. 2003). The parallel-plate capacitor with electrostatic actuation that is preferable due to its high self-resonance, high quality factor, and low power consumption and the interdigitated capacitors that have a linear response, but exhibit a low self-resonance and low quality factor. Comb drive structures can be widely used in electrostatically actuated MEMS devices. In this paper, we present a surface-micromachined variable capacitor that employs comb drive actuators to vertically displace parallel plate capacitors.

The main aim of this article is to introduce a new structure to achieve variable capacitor with large tuning range using electrostatic actuators. The main problem in the electrostatic type variable capacitor is the pull in instability. This phenomenon limits the range of tuning

✉ Saeid Afrang
afrang1@yahoo.com

¹ Department of Electrical Engineering, Urmia University, Urmia, Iran

(Azizi et al. 2018). We have proposed a new structure to overcome this problem, and achieve large tuning range. Based on the proposed structure, we have introduced two steps to postpone pull in instability point. At the first step and for the first time we have used vertical comb drive electrostatic actuator as a variable capacitor. In the comb drive electrostatic actuators, the pull in instability occurs later than conventional parallel plate electrostatic actuators. Therefore, the tuning range of the variable capacitor is increased. In the second step, to increase more tuning range, the auxiliary cantilever beams are added. These beams are located in the pull in instability location due to first step. The beams increase the stiffness of the structure and for the second time postpone pull in instability location.

2 Device structure

The schematic diagram of the proposed structure is shown in Fig. 1. The structure consists of movable and fix comb drives, auxiliary cantilever beams, anchors, fixed-guided end beams as springs and two parallel plates. The lower plate is fixed and upper plate is suspended by fixed-guided end beam. The electrostatic comb drive actuator is used to move upper plate downward. The comb drives are connected to the sides of the upper plate. The movable plate together with fixed plate makes the proposed variable capacitor. The four auxiliary cantilever-beams are located under the upper movable plate. These beams increase the tunability range of the variable capacitor. When the actuation voltage is applied to the comb drives, the electrostatic force generated in the comb drives moves the upper plate downward. This generated electrostatic force is more linear than the conventional electrostatic force, produced by the parallel-plate actuator. Moreover, this technique postpones the pull-in behavior compared to conventional parallel-

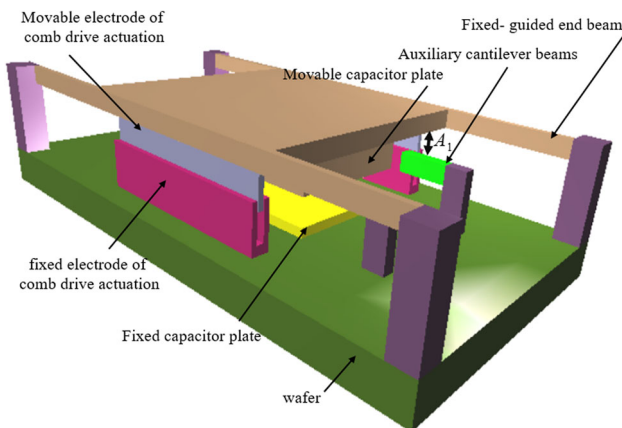


Fig. 1 The schematic diagram of the proposed variable capacitor

plate capacitors. Therefore, allows the movable plate to continue moving down linearly and consequently increase the tunability range of the variable capacitor. In the pull in point the equivalent stiffness of the structure becomes zero and leads the system to an unstable condition by undergoing to a saddle node bifurcation. In the proposed structure to avoid pull-in instability and increase the capacitance tuning range, mechanical stiffness of the structure is increased by changing boundary conditions by locating an auxiliary cantilever beam under the movable plate.

3 Design

The aim of this research is to introduce electrostatic comb drive as a vertical actuator to create variable capacitor with maximum tuning range. Figure 2 shows the comb drive architecture.

As shown in Fig. 2a, when the voltage is applied, the movable comb will be displaced in the Z direction due to the fringing fields created in the comb.

The capacitance between electrically conductive combs is expressed as:

$$C_{comb-drive} = N\epsilon_0 h(z + w_0) \left(\frac{1}{g - y} + \frac{1}{g + y} \right). \quad (1)$$

For equal distance between the plates the capacitance is expressed as:

$$C_{comb-drive} = N\epsilon_0 h(z + w_0) \left(\frac{2}{g} \right). \quad (2)$$

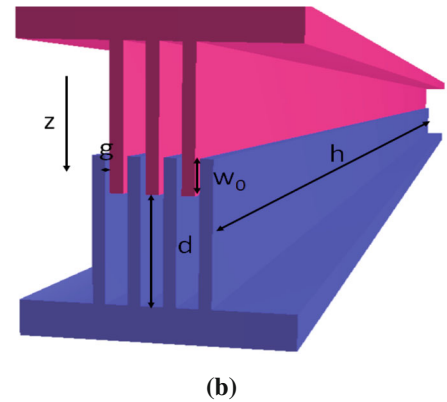
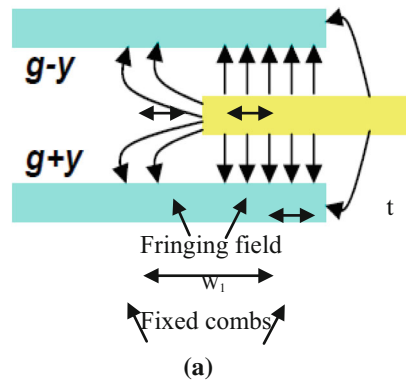
In Eq. 2 ‘N’ indicates the number of combs, ‘h’ refers to the comb-length, ‘w₀’ is the initial overlap, ‘g’ is the adjacent gap size, ‘z’ is the vertical displacement amplitude along the z axis and ‘y’ represents the transversal displacement along the y axis. The electrostatic force applied to the comb drive is found by considering the power delivered to a time dependent capacitance and is given by: (Legtenberg et al. 1996; Jaecklin et al. 1992; Chen et al. 2004).

$$\begin{aligned} F_{z1} = F_f &= \frac{1}{2} V^2 \frac{dC_{comb-drive}(z)}{dz} = \frac{1}{2} \frac{d}{dz} \left[N\epsilon_0 h(z + W_0) \frac{2}{g} \right] \\ &= \frac{N\epsilon_0 h}{g} V^2. \end{aligned} \quad (3)$$

The movable electrode on ground potential will be displaced in the z direction due to the fringe fields created in the comb. There is another capacitor which consists of the capacitor plate formed by the front end of the movable fingers and of the parallel part of the fixed electrode in front of it. This capacitance is expressed as:

Fig. 2 Comb drive structure

Movable comb →



$$C_{parallel-plate} = 2N\epsilon_0 \frac{A}{(d-z)}, \tag{4}$$

where ‘A’, ‘N’ and ‘d’ are the electrostatic area, number of fingers, and initial distance of the front ends of the fingers if no actuation occurs and ‘z’ refers to the displacement in the z direction, respectively. The capacitor named by parallel plate capacitor does not have same electrodes. If we consider the electrostatic area of the front end of the movable fingers by $A_1 = h * t$, and the parallel part area of the fixed electrode in front of movable electrode by $A_2 = h * w_1$, then the capacitance is expressed as:

$$C_{parallel-plate} = 4N\epsilon_0 \frac{A_1 A_2}{(d-z)(A_1 + A_2)}. \tag{5}$$

The corresponding parallel plate electrostatic force is given by:

$$F_{z2} = F_p = \frac{1}{2} V^2 \frac{dC_{parallel-plate}(z)}{dz} = 2N\epsilon_0 \frac{A_1 A_2}{(d-z)^2 (A_1 + A_2)} V^2. \tag{6}$$

For an actuator in equilibrium, two types of electrostatic forces can be stated. The total electrostatic force in the comb drive is expressed as:

$$F_e = F_f + F_p = \frac{N\epsilon_0 h}{g} V^2 + 2N\epsilon_0 \frac{A_1 A_2}{(d-z)^2 (A_1 + A_2)} V^2. \tag{7}$$

If the movable electrode is displaced following Hooke’s law, the reaction force F_s , is generated:

$$F_s = k_z(d-z). \tag{8}$$

In this equation ‘ k_z ’ refers to equivalent spring constant in the ‘z’ direction. The spring constant without auxiliary cantilever beams is due to four fixed-guided end beams. These beams connect upper plate to anchors.

Corresponding equation of this spring constant is given by (Roack et al. 1975):

$$k_{1z} = 4 \frac{Ewt^3}{l^3}. \tag{9}$$

The spring constant of four auxiliary cantilever beams for a concentrated load is given by (Roack et al. 1975):

$$k_{2z} = \frac{Ewt^3}{l^3}. \tag{10}$$

For both equation ‘w’, ‘t’ and ‘l’ are width, thickness and length of the beams, respectively.

When the upper plate touches the auxiliary cantilever beams, the equivalent spring constant is parallel combination of four fixed-guided beams with four auxiliary cantilever beams. As it is seen, auxiliary cantilever beams increase equivalent mechanical stiffness of the structure with respect to electrical stiffness. Therefore pull in phenomenon is postponed and capacitance tuning range is increased. Another method to postpone pull in phenomenon is to increase lateral electrostatic force with respect to parallel electrostatic force. From Eq. 7 if the generated lateral electrostatic force F_f is the dominated force compared to F_p then pull in phenomenon is postponed.

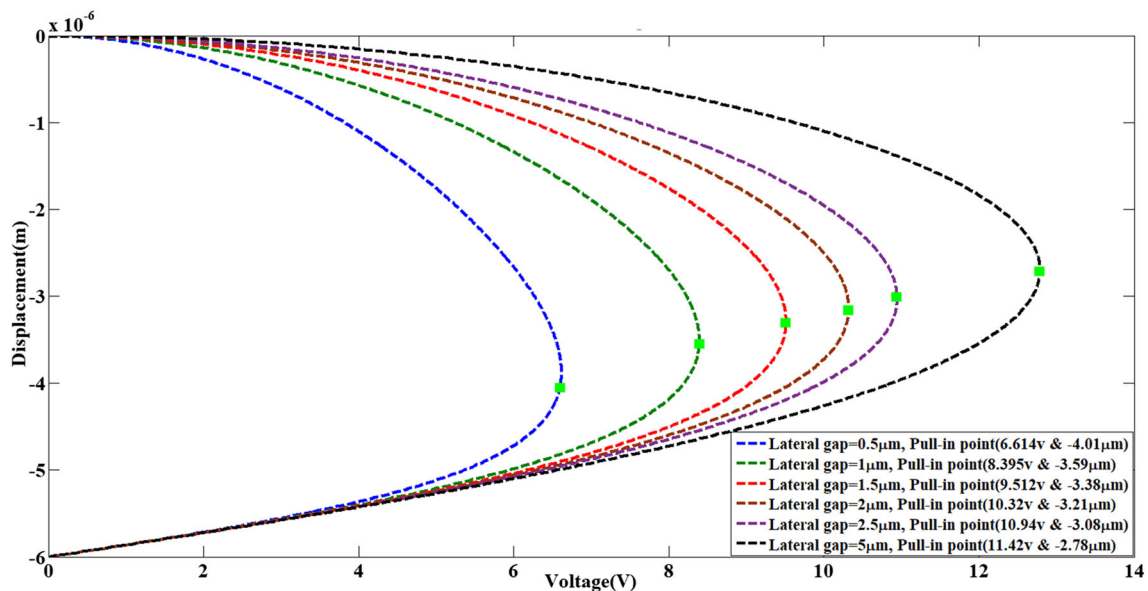
4 Calculation and simulation results

At the first step, the proposed structure is calculated for different comb drive plate gaps without auxiliary cantilever beams using MATLAB software. Materials and geometrical parameters of the structure are indicated in Table 1.

Figure 3 shows calculation results of movable comb drive displacement versus applied voltage for different comb drive plate gaps without auxiliary cantilever beam. From Fig. 3 smaller comb drive plate gaps increase the linear region and consequently capacitance tuning range.

Table 1 Materials and geometrical parameters

Parameters	Value	Parameters	Value
Young's modulus (Al)	77 Gpa	Length of fixed-guided end beam	500 μm
Initial distance of the front ends of the fingers	6 μm	Width of fixed-guided end beam	25 μm
Initial air gap of variable capacitor	6 μm	Thickness of fixed-guided end beam	2 μm
Length of auxiliary cantilever beams	190 μm	Length of combs	800 μm
Width of auxiliary cantilever beams	50 μm	Width of combs	3 μm
Thickness of auxiliary cantilever beams	2 μm	Combs thickness	2 μm
Yield strength (Al)	310 MPa	Variable capacitor area	600 \times 800 μm^2

**Fig. 3** Effect of different comb drive plate gaps in the pull in situation without auxiliary cantilever beam

To verify, the proposed structure is simulated for different comb drive plate gaps using intellisuite software. Figure 4 shows simulation results of movable comb drive displacement versus applied voltage for different comb drive plate gaps.

The calculated and simulated results of different lateral gaps are shown in Table 2.

From the table, the calculation results for the comb drive location in the pull in point due to different lateral gaps are approximately same as simulation results.

Based on compared results, the corresponding pull in voltages of calculation and simulation of different lateral gaps are not equal. Figure 5 describes the mentioned difference. In this figure, “ g ” is the lateral gap between movable and fixed fingers and “ d_0 ” is the initial gap between the front end of the movable fingers and of the parallel part of the fixed electrode in front of it. As shown in Fig. 5a, for $g \ll d_0$, fringe field appears in front of movable finger. Due to the fringing field, the electrostatic

area is smaller than A_1 in Eq. 5. Therefore, the amount of calculated pull in voltage is smaller than simulation. For $g \geq d_0$, as shown in Fig. 5b, the electrostatic area with initial gap distance “ d_0 ” is increased. This electrostatic area is more than A_1 in Eq. 5. In this case, the amount of calculated pull in voltage is more than simulated one.

In the next step, to increase the capacitance tuning range, the auxiliary cantilever beam is added. The beam is located in the pull in point under the upper plate. This point for one micrometer comb drive plate lateral gap and two micrometer comb thickness is 3.5 $\hat{\mu}\text{m}$ distance from the upper plate. Figure 6 shows calculated result of the proposed structure with added auxiliary beam.

From the figure the second pull in point is 4.44 $\hat{\mu}\text{m}$ distance from the upper plate.

It is seen that the pull in point is postponed and working range as a capacitor is increased. Increased working range increases the tuning range.

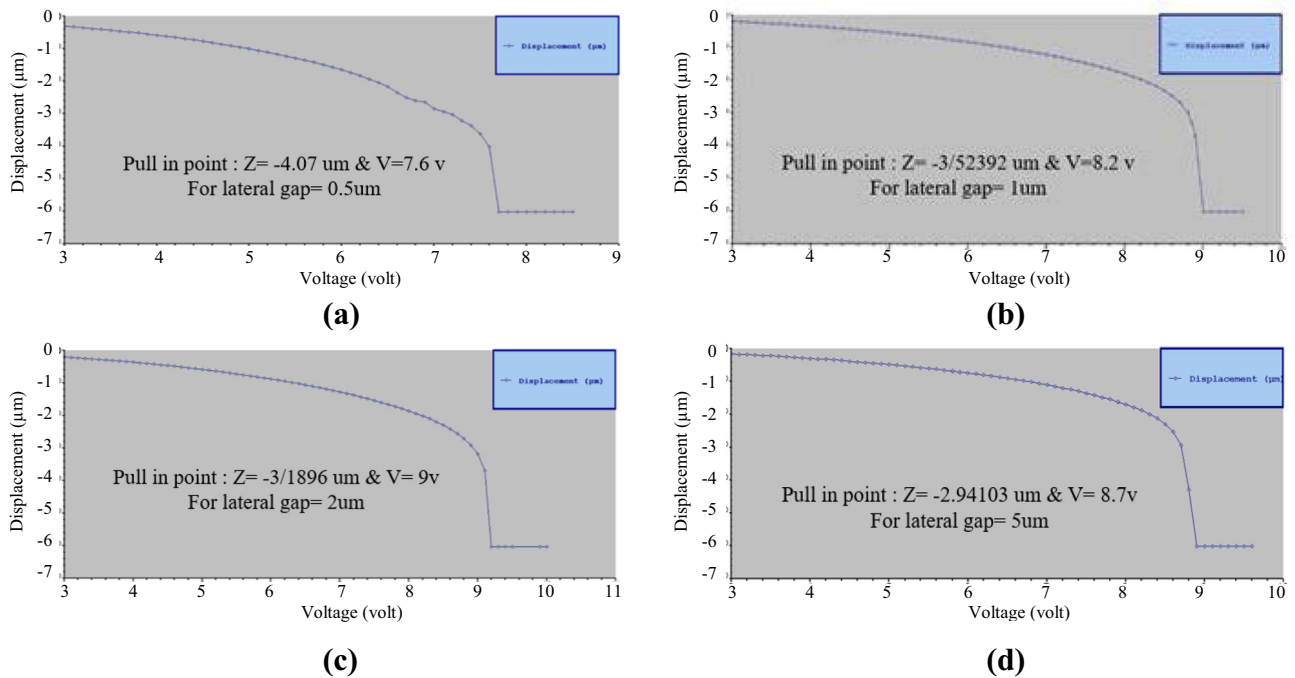


Fig. 4 Simulation results of movable comb drive displacement versus applied voltage for different comb drive plate gaps

Table 2 The calculated and simulated results of different lateral gaps

Lateral gap (μm)	Pull in point (volt- μm) calculation	Pull in point (volt- μm) simulation
0.5	6.6–4	7.6–4
1	8.4–3.6	8.2–3.5
1.5	9.5–3.4	8.7–3.3
2	10.3–3.2	9–3.2
5	11.4–2.8	8.7–2.9

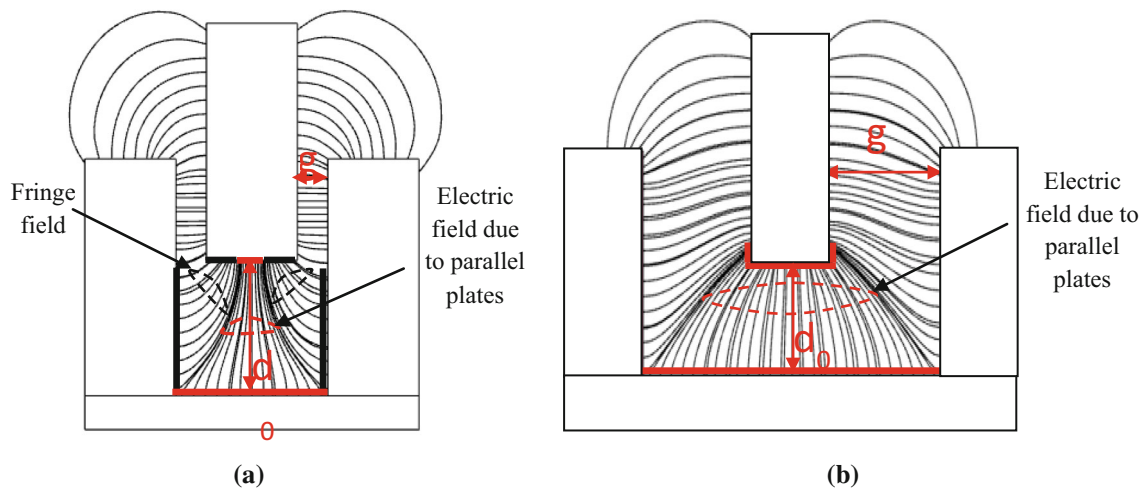


Fig. 5 Electric field distribution in the comb drive actuator a $g \ll d_0$, b $g \geq d_0$

To verify, the proposed structure is simulated using Intellisuite software. Figure 7 shows simulation result of the proposed structure with added auxiliary beam. From

this figure, the second pull in point is $4.62 \hat{A}\mu\text{m}$ distance from the upper plate. As it is seen, in the final structure, the

Fig. 6 Calculation result of the proposed structure with added auxiliary beam

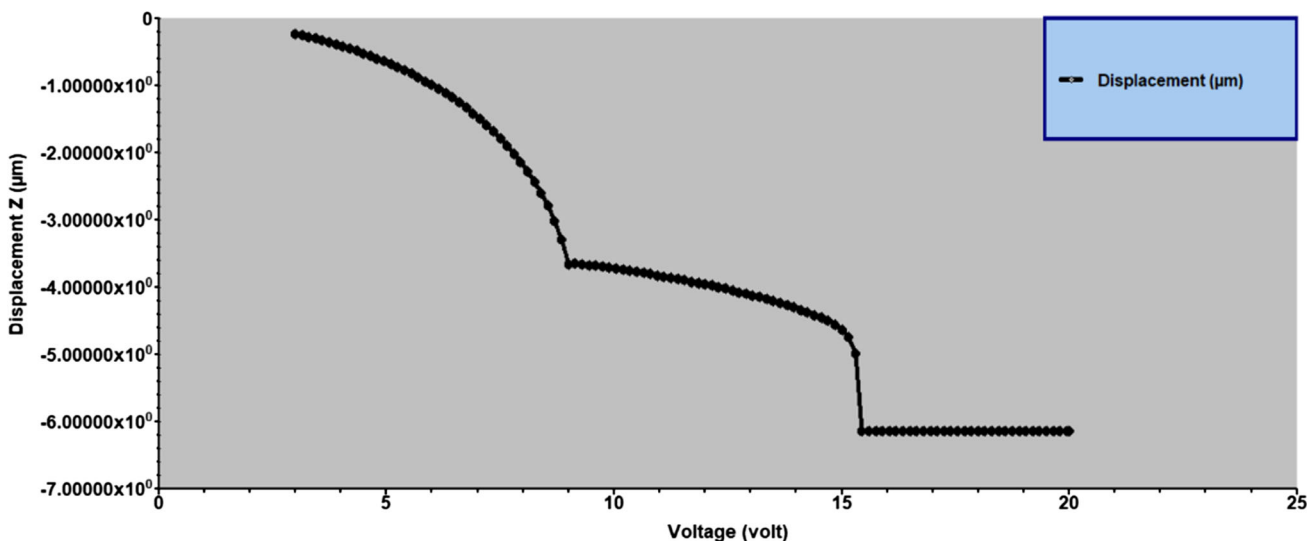
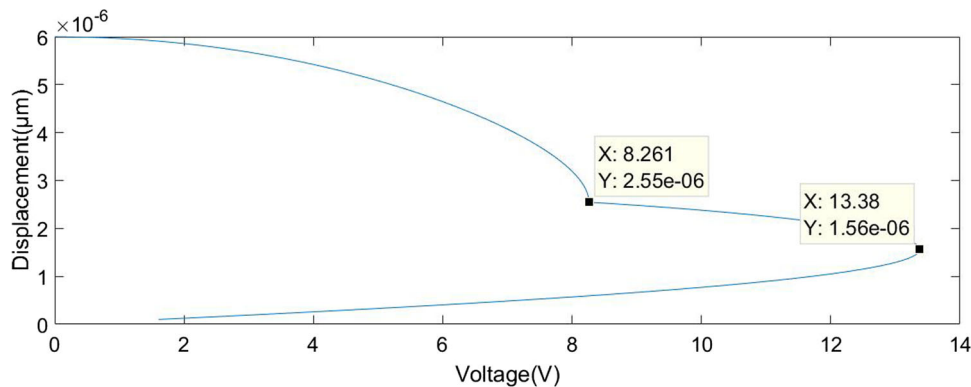


Fig. 7 Simulation result of the proposed structure with added auxiliary beam

results of the numerical solution are approximately same as simulation results.

5 Tuning range and lateral instability

Tuning range is the ratio of variable capacitor’s maximum changed capacitance to the minimum capacitance, defined as:

$$\text{Tuning range} = \frac{C_{\max} - C_{\min}}{C_{\min}} \times 100. \tag{11}$$

Considering the plates area, initial and final air-gap of variable capacitor, the minimum and maximum capacitance is 0.71 PF and 2.74 PF, respectively. The tuning range for the final structure by considering the minimum and maximum capacitances is 285%. The fringing field is not considered at this step. Figure 8 shows calculated result of capacitance versus different applied voltages with added auxiliary beams. To verify, the proposed structure is simulated using Intellisuite software. Figure 9 shows

simulation result of the proposed structure with added auxiliary beam. From this figure, and due to fringing field effect, the simulated capacitance is not same as calculated one.

The tuning range for the final structure by considering the minimum and maximum capacitances is 285%.

The lateral instability occurs when the electrostatic stiffness transverse to the axial direction of motion exceeds the transverse mechanical stiffness of the suspension (Legtenberg et al. 1996; Elata et al. 2003). Therefore, the most common way to avoid it is by increasing the transverse stiffness of the suspension (Bryzek et al. 2003; Chen et al. 2004; Grade et al. 1999).

The equivalent spring constant equations of four fixed-guided end beams in the “x” and “y” directions are as below:

$$k_{1y} = 4 \frac{Etw^3}{l^3}, \tag{12}$$

$$k_{1x} = 4 \frac{Etw}{l}. \tag{13}$$

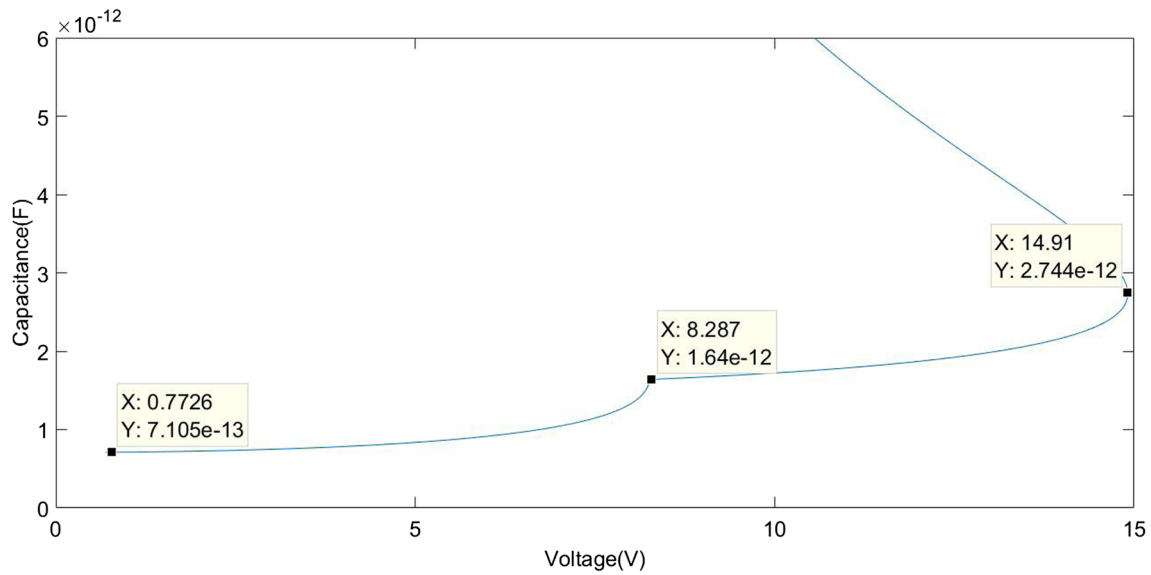
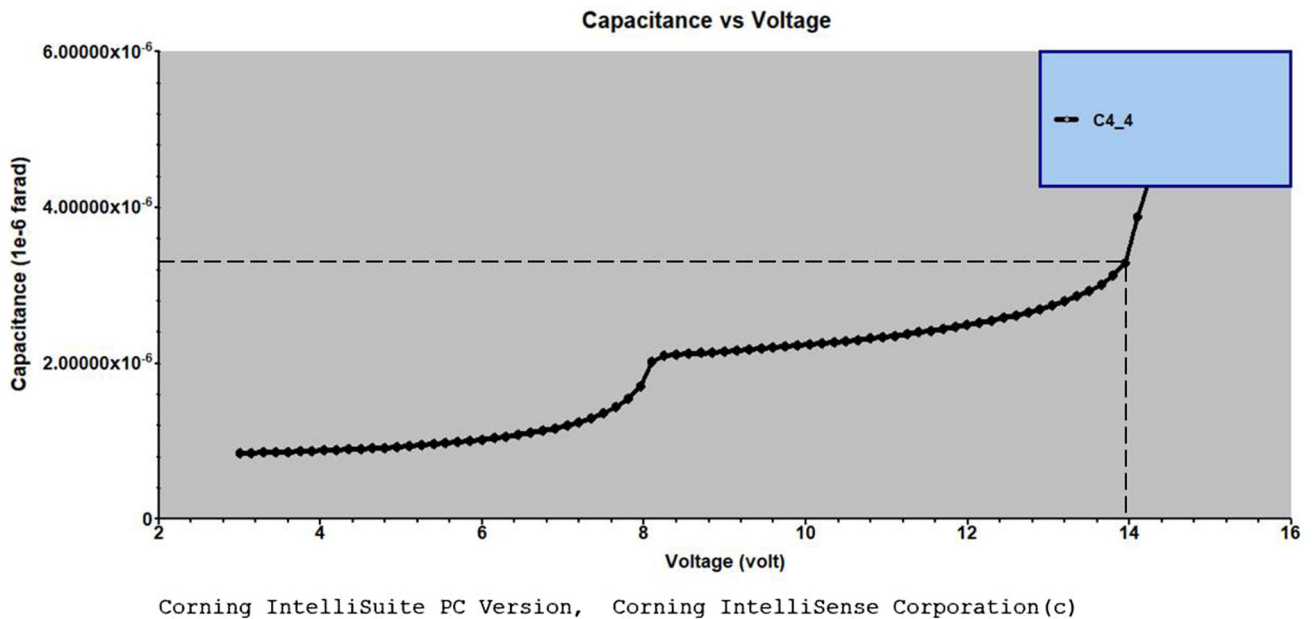


Fig. 8 Calculated result of capacitance versus different applied voltages with added auxiliary beam



Corning IntelliSuite PC Version, Corning IntelliSense Corporation(c)

Fig. 9 Simulated result of capacitance versus different applied voltages with added auxiliary beam

From Table 1, and Eqs. 9, 12 and 13, the equivalent spring constant of the fixed- guided end beams in the “x”, “y” and “z” directions are 30800, 77 and 0.5, respectively. As it is seen, the spring constant in the “x” and “y” directions are much larger than “z” direction.

Finally, to know the maximum induced stress in the structure, the maximum voltage is applied to the combs. Figures 10 and 11 show the maximum displacement (6 μm) of the movable plate and stress induced in the structure due to maximum applied voltage. From Fig. 11, the maximum induced stress is 11.5 MPa. This stress is much smaller than yield strength of aluminum.

Table 3 shows MEMS variable capacitor performance comparison with the previously published variable capacitors. This comparison indicates a significantly high quality in tenability and actuation voltage for the new design.

6 Proposed fabrication process

The fabrication process starts with selection of a high resistance substrate to prevent electrical connection between the different parts of the structure. Then, 0.1 μm layer of Al is deposited by sputtering and patterned to

Fig. 10 Schematic of the structure for maximum displacement

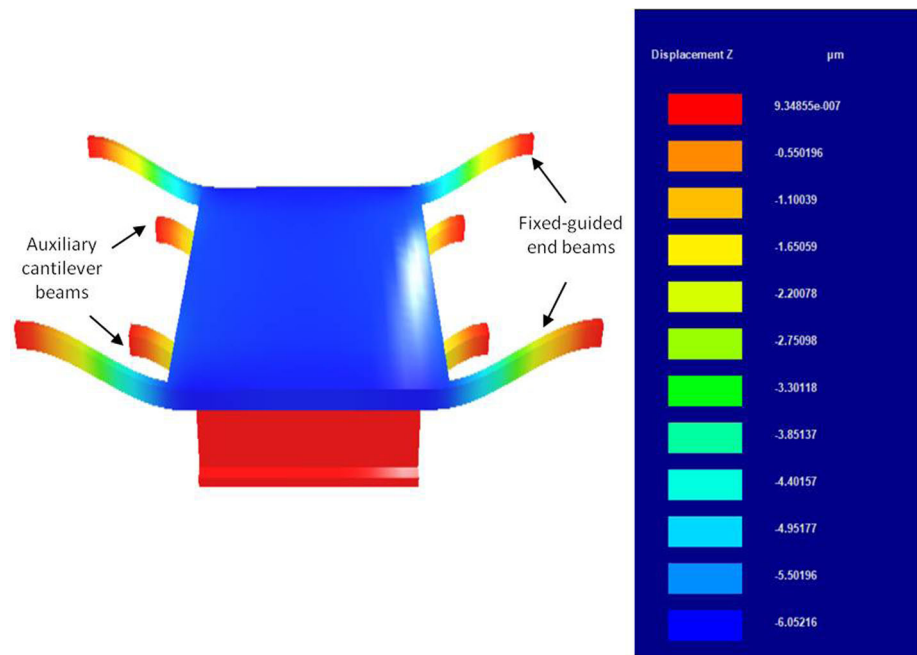


Fig. 11 The stress induced in the structure

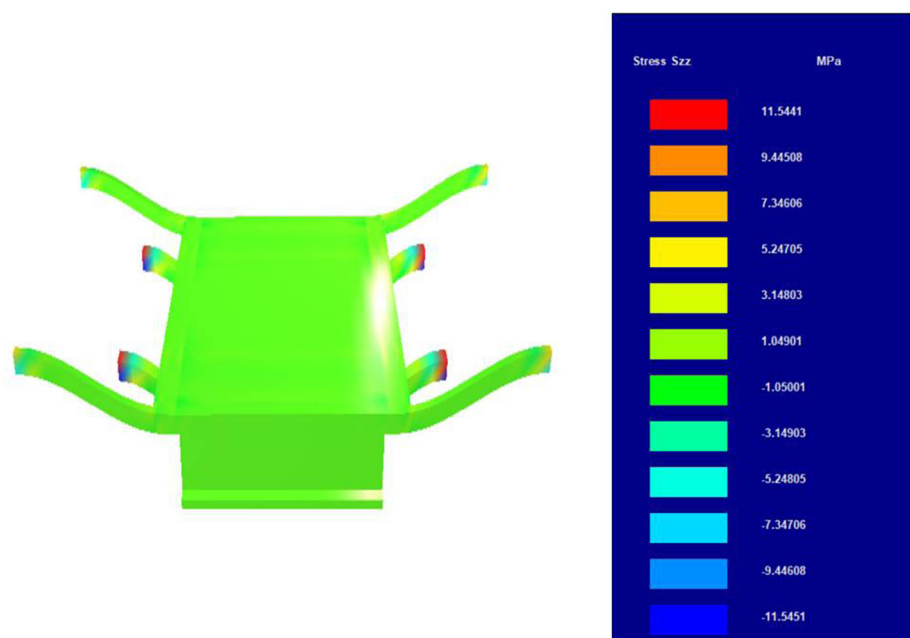


Table 3 Comparison of current state of the art MEMS based variable capacitors

	C_{\min} (PF)	C_{\max} (PF)	Tunability (%)	Actuation voltage (V)
Mobki et al.	24.5	49	100	41
Afrang et al.	24.5	75.6	207	40
Zhu et al. (2010)	118	551	367	120
This work	0.71	2.74	285	14

define lower plate of capacitor, anchors of fixed-guided end beams and fixed combs as shown in Fig. 12a. Next, a 0.1 μm silicon–Nitride as a dielectric layer is deposited and

patterned as shown in Fig. 12b. In the third step a 6 μm polyimide 2526 as a sacrificial layer is deposited and patterned, to define fixed combs by aluminum electroplating

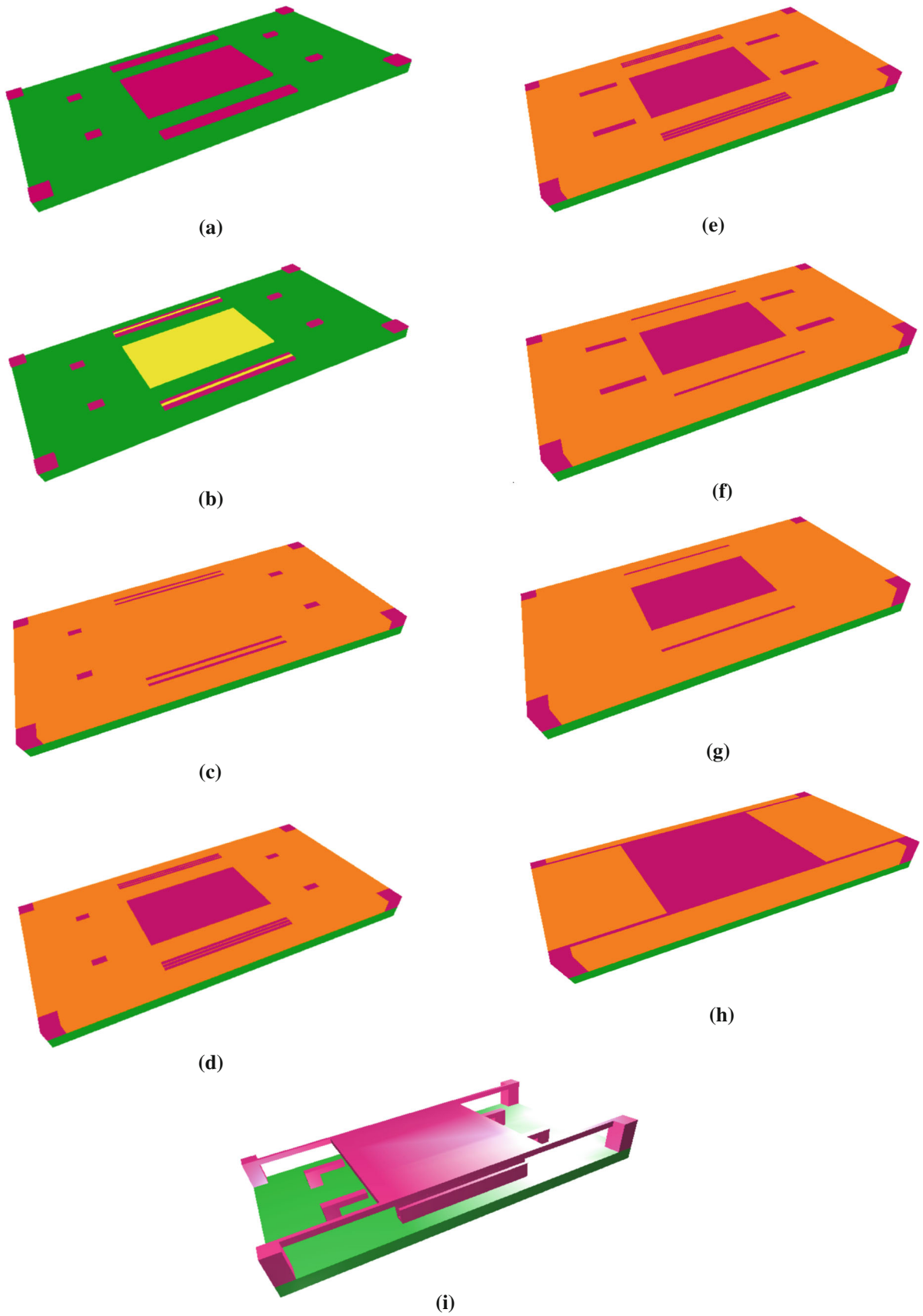


Fig. 12 Proposed fabrication process

(Fig. 12c). Then 0.5 μm aluminum is deposited and patterned to create upper plate of capacitor, anchors of fixed-guided end beams and overlap region of fixed and movable combs (Fig. 12d). To create the same level the other area in step four is filled with polyimide 2526. In the next step 0.5 μm polyimide 2562 as a sacrificial layer and as a mold for aluminum electroplating is deposited patterned and electroplated to define upper plate of variable capacitor, overlap region of fixed and movable combs, anchors of fixed-guided end beams and auxiliary cantilever beams (Fig. 12e). Again in the sixth step 1.5 μm polyimide 2562 as a sacrificial layer and as a mold for aluminum electroplating is deposited patterned and electroplated to define upper plate of variable capacitor, movable combs, anchors of fixed-guided end beams and auxiliary cantilever beams. The thicknesses in the previous and this step determine the auxiliary cantilever beam thickness (Fig. 12f). Then a 4.5 μm polyimide 2526 as a sacrificial layer and as a mold for aluminum electroplating is deposited patterned and electroplated to define upper plate of variable capacitor, movable combs, and anchors of fixed-guided end beams (Fig. 12g). In the eighth step, a 2 μm aluminum is deposited and patterned to define upper plate of variable capacitor, fixed-guided end beams and anchors of fixed-guided end beams (Fig. 12h). Finally, isotropic plasma ashing is used to remove sacrificial layer (Fig. 12i).

7 Conclusion

A new structure to increase the capacitance tuning range was proposed. The pull in point of vertical electrostatic comb drive actuator was investigated. It was shown, the gap between the combs affect the pull in point and consequently linear traveling range of the movable capacitor plate. Based on the research, smaller gaps increased the capacitor tuning range. On the other hand, added auxiliary beams more increased the tuning range of the variable capacitor. The proposed structure was designed and then tested with MATLAB software. To verify, the structure was simulated using Intellisuite software. The achieved maximum tuning range in the proposed structure is 285%.

References

- Afrang S, Rezazadeh Gh, Mobki H (2015) A new MEMS based variable capacitor with wide tunability, high linearity and low actuation voltage. *J Microelectron* 46(2):191–197
- Azizi A, Malekzadeh N, Mobki H, Arbi A (2018) Bifurcation behaviour and stability analysis of a nano-beam subjected to electrostatic pressure. *Appl Comput Math* 7(1–2):1–11
- Bakri-Kassem M, Mansour R (2004) An improved design for parallel plate mems variable capacitors. In: *Microwave symposium digest*, IEEE MTT-S international, 2:865–868
- Bakri-Kassem M, Mansour R (2004b) Two movable-plate nitride-loaded mems variable capacitor. *Microwave theory and techniques*. *IEEE Trans* 52(3):831–837
- Bakri-Kassem M, Mansour R (2006) High tuning range parallel plate mems variable capacitors with arrays of supporting beams. In: *Micro electro mechanical systems, MEMS Istanbul*. 19th IEEE international conference on, pp 666–669
- Borwick I, Stupar P, DeNatale J, Anderson R, Erlandson R (2003) Variable mems capacitors implemented into RF filter systems. *Microwave theory and techniques*. *IEEE Trans* 51(1):315–319
- Bryzek J, Abbott E, Flannery A, Cagle D, Maitan J (2003) Control issues for MEMS. In: *Proceedings of the 42nd IEEE conference on decision and control*, vol 3, pp 3039–3047. 9–12 Dec 2003
- Chen C, Lee C (2004) Design and modeling for comb drive actuator with enlarged static displacement. *Sens Actuators* 115(2–3):530–539
- Dec A, Suyama K (2000) Micromachined electro-mechanically tunable capacitors and their applications for RF IC's. *IEEE J Solid State Circ* 35(8):1231–1237
- Elata D, Bochobza-Degani O, Nemirovsky Y (2003) Analytical approach and numerical alpha-lines method for pull-in hypersurface extraction of electrostatic actuators with multiple uncoupled voltage sources. *J Microelectromech Syst* 53:681–691
- Faheem F, Hoivik N, Lee Y, Gupta K (2003) Post-enabled precision flip-chip assembly for variable mems capacitor. In: *Microwave symposium digest*, 2003 IEEE MTT-S International, 3:1927–1930
- Jaeklin VP, Linder C, De Rooij N F, Moret JM (1992) Micromechanical comb actuators with low driving voltage. *J Micromech Microeng* 2:250–255
- Legtenberg R, Groeneveld A, Elwenspoek M (1996) Comb-drive actuators for large displacements. *J Micromech Microeng* 53:320–329
- Li Z, Tien NC (2002) A high tuning-ratio silicon micromachined variable capacitor with low driving voltage. *Solid State Sens Actuat Microsyst* 13(3):239–242
- Mobki H, Sadeghi M, Afrang S, Rezazadeh G (2011) On tenability of a MEMS based variable capacitor with a novel structure. *Microsyst Technol* 17:1447–1452
- Nguyen C, Katehi L, Rebeiz G (1998) Micromachined devices for wireless communications. *IEEE* 86(8):1756–1768
- Nguyen H, Hah D, Patterson P, Wu M (2002) A novel MEMS tunable capacitor based on angular vertical comb drive actuators. *Solid-state sensor, actuator and microsystems* 13(3):277–280
- Nguyen H, Hah D, Patterson P, Chao R, Piyawattanametha W, Lau E, Wu M (2004) Angular vertical comb-driven tunable capacitor with high-tuning capabilities. *Microelectromech Syst J* 13(3):406–413
- Peroulis D, Katehi L (2003) Electrostatically-tunable analog RF MEMS varactors with measured capacitance range of 300%. In: *Microwave Symposium Digest*, 2003 IEEE MTT-S International, 3(8–13):1793–1796
- Rijks T, Beek J, Steeneken P, Ulenaers M, De Coster J, Puers R (2004) RF MEMS tunable capacitors with large tuning ratio. In: *MicroElectro mechanical systems*, 17th IEEE International Conference on. (MEMS), pp 777–780
- Roack R, Young W (1975) *Formulas for stress and strain*. McGraw Hill, New York
- Yao J, Park S, Anderson R, DeNatale J (1998) High tuning ratio MEMS-based tunable capacitors for RF communications. *Solid-state Sensor and Actuator Workshop*, Hilton Head Island, pp 124–127

- Yao J, Park S, DeNatale J (2000) A low power/low voltage electrostatic actuator for RF MEMS applications. Proceedings of Solid-state Sensor and Actuator Workshop, Hilton Head Island, pp 246–249
- Young D, Boser B (1996) A micromachined variable capacitor for monolithic low-noise VCOs. In: Proceedings of IEEE solid-state sensors actuators workshop, Hilton Head, SC, pp 86–89
- Young D, Tham J, Boser B (1999) A micromachine-based low phase-noise GHz voltage-controlled oscillator for Wireless communications. In: The 10th international conference on solid-state sensors and actuators (Transducers'99), Sendai, Japan, 19, 11(5):285–300
- Zhu Y, Yuce MR, Moheimani (2010) A low loss MEMS tunable capacitor with movable dielectric. In: IEEE sensors 2009 conference, pp 651–654
- Zou J, Liu C, Aline J, Chen J, Kang S (2000) Development of a wide tuning range MEMS tunable capacitor for wireless communication systems. In: IEEE IEDM, pp 403–406

Publisher's Note Springer Nature remains neutral with regard to jurisdictional claims in published maps and institutional affiliations.